WHEEL TRACK TESTING AND FINITE ELEMENT ANALYSIS OF CONCRETE BLOCK PAVEMENTS

L.J.M. Houben and M.M.J. Jacobs

Delft University of Technology, Delft, The Netherlands

SUMMARY

This paper describes an investigation into the structural behaviour of six concrete block pavements, tested by means of a wheel track apparatus that recently has been installed at the pavement test area outside the Road and Railroad Research Laboratory of the Delft University of Technology. The pavement structures (total thickness 1.23 m) consisted of rectangular concrete paving blocks (thickness 80 mm) in herringbone bond, 50 mm crushed sand bedding layer, a crushed concrete unbound base (thickness 0,100, 200 or 300 mm) and a Eastern Scheldt sand sub-base. The test sections were subjected to 275,000 6 kN wheel load repetitions.

The fundamental stress-dependent resilient and permanent deformation behaviour of the applied unbound materials was determined by means of cyclic loading tri axial tests. The measurements on the test sections (falling weight deflection measurements and rutting measurements) showed a substantial positive effect of the crushed concrete unbound base.

A two-dimensional finite element analysis of the test sections' resilient behaviour clearly showed the 'progressive stiffening' behaviour of all test sections. On basis of this rough finite element analysis and supplementary linear-elastic multilayer calculations, permanent deformation coefficients were determined for all unbound layers of the test sections by means of the 'progressive stiffening' theory developed earlier on by the Delft University of Technology.

A more advanced, but also more (computer)time consuming axial-symmetric finite element analysis, including the stress-dependent resilient behaviour of the applied unbound materials, yielded detailed information with respect to the distribution of resilient moduli and stresses within some of the test pavement structures. Finally a very good correspondence was found between the measured rutting and the rutting, calculated on basis of this axial-symmetric finite element analysis and the stress-dependent permanent deformation behaviour of the applied unbound materials.

1. INTRODUCTION

In 1985 a wheel track apparatus has been installed at the pavement test area outside the Road and Railroad Research Laboratory of the Delft University of Technology.
In the first instance six concrete block pavements were tested by means of this wheel track apparatus (1,2). The main objective of this research was to quantify the effect of an unbound base on the structural behaviour of concrete block pavements. Therefore the six test sections only differed with regard to the thickness of the crushed concrete base. The concrete block test sections were subjected to 275,000 6 kN wheel load repetitions.

This paper describes the structural behaviour of the concrete block test sections as well as the analysis of this performance on basis of both two-dimensional and axial-symmetric finite element calculations.
First the chapters 2 and 3 give a short description of the Delft wheel track apparatus and the pavement structure of the six concrete block test sections.
In chapter 4 the measured resilient and permanent deformation behaviour of both the unbound materials, applied in the pavement structures, and the concrete block test sections will be described.
In chapter 5 first a two-dimensional finite element analysis of the test sections' resilient deformation (deflections) behaviour is made. On basis of this analysis, supplementary linear-elastic multilayer calculations and the permanent deformation (rutting) behaviour of the test sections, for all unbound layers in the test sections permanent deformation coefficients will be derived by means of the 'progressive stiffening' theory developed earlier on by the Delft University of Technology.
In chapter 6 first an axial-symmetric finite element analysis of the test sections' resilient deformation behaviour is given, making allowance for the stress-dependent resilient deformation behaviour of the unbound materials applied in the pavement structures. Finally for some test sections the progress of rutting will be calculated from this finite element analysis and the stress-dependent permanent deformation behaviour of the applied unbound materials.

2. WHEEL TRACK APPARATUS

The carrousel-type Delft wheel track apparatus is a welded steel construction, consisting of eight beams (figure 1). At each beam a little wagon with rubber tyre is fixed. By means of steel plates each tyre can be loaded up to P - 6 kN; the tyre pressure p = 0.6 N/mm^2. The maximum running speed is 10 km/h.

By means of a conducting-rail and a special transit-construction on each beam, each tyre is forced to run a hexagonal track in stead of a circular track. The conducting-rail was constructed in such a way that on each side of the hexagon

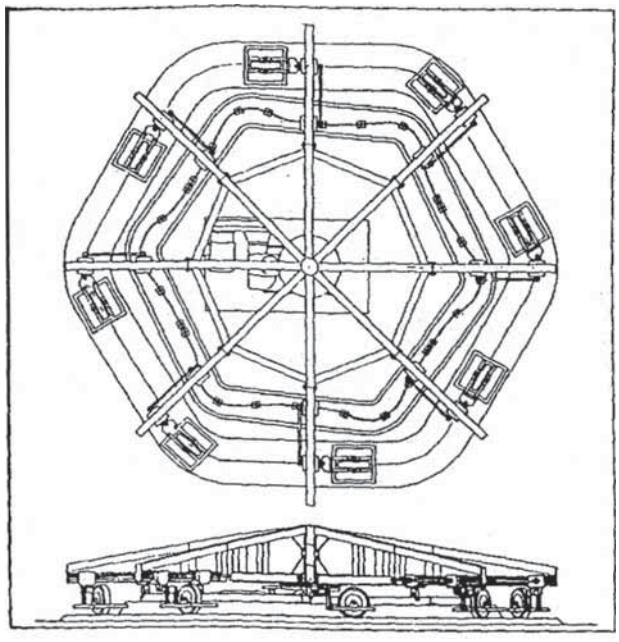


Figure 1. The Delft wheel track apparatus.

the tyre runs a straight line over a distance of about 2 m.

In the wheel track apparatus, six sections with different pavement structures can be tested at the same time. In the investigation described here, the test sections were subjected to 275,000 repetitions of the 6 kN wheel load.

3. TEST PAVEMENTS

The main objective of the research by means of the Delft wheel track apparatus was the determination of the effect of an unbound base on the structural behaviour of concrete block pavements. Therefore the only difference between the six concrete block test sections was the thickness of the unbound base. Crushed concrete was applied as unbound base material.
The pavement structure of the six test sections was as follows (figure 2):

- rectangular concrete paving blocks, nominal thickness h_1 - 80 mm, in herringbone bond
- bedding layer, thickness h_2 = 50 mm, of crushed sand
- unbound base of crushed concrete, thickness h_3 according to table 1
- unbound sub-base of Eastern Scheldt sand, thickness h_4 according to table 1
- subgrade, consisting of about 1.5 m Eastern Scheldt sand on clay.

On all the test sections the total thickness of the pavement structure (h_1 through h_4) was 1.23 m.

The mean dimensions of the rectangular concrete paving blocks were: length 210.1 mm, width 104.8 mm and thickness 81.2 mm. The mean joint width was 2.1 mm.

The gradings of the crushed sand, the crushed concrete and the Eastern Scheldt sand are shown in figure 3. These gradings meet the Dutch requirements (3) for bedding sand, unbound base material (nominal grading 0/40 mm) and sub-base material respectively.

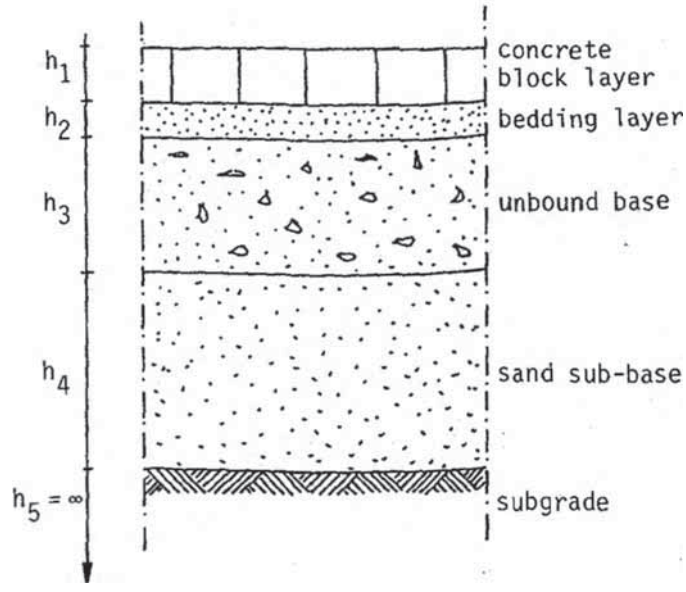


Figure 2. Concrete block pavement structure.

section	unbound base thickness h_3 (mm)	sand sub-base thickness h_4 (mm)
1	0	1100
2	100	1000
3	200	900
4	300	800
5	200	900
6	0	1100

Table 1. Thickness of unbound base and sand sub-base in the six concrete block test sections .

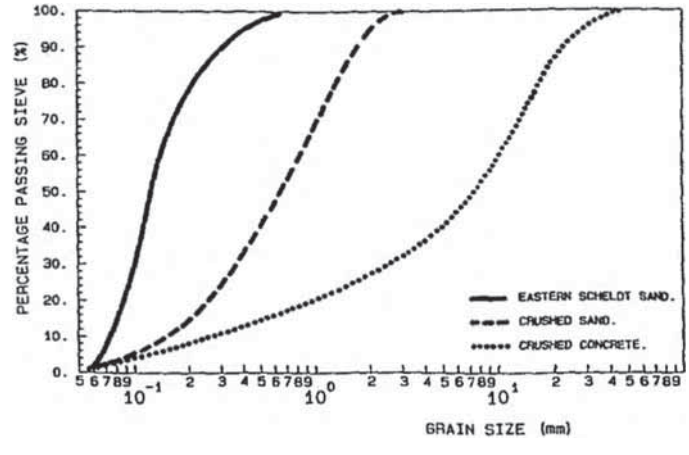


Figure 3. Gradings of the unbound materials applied in the six concrete block test sections.

The mean in situ dry density of the crushed concrete base material, as determined by means of the 'sand replacement' method (3), was 93.3 per cent of modified mpd (maximum proctor density). The mean in situ water content was 6.9 per cent.

In the test sections 2 through 5 the mean in situ dry density of the Eastern Scheldt sand sub-base material was 100.1 per cent mpd, the mean in situ water content was 8.6 per cent. However, the mean in situ dry density of the Eastern Scheldt sand in the sections 1 and 6 was only 96.7 per cent mpd, with a mean water content of 8.2 per cent.

4. TEST RESULTS

4.1. Cyclic loading tri axial tests

In order to obtain fundamental stress/strain parameters for the unbound materials applied in the test sections, cyclic loading tri axial tests were carried out. The apparatus used for these tests has a sample size of 400 mm x 800 mm. The apparatus is a constant confining pressure tri axial set-up (4).

Figure 4 shows the stresses applied to the tri axial specimen in the cyclic loading tests. The constant, all around confining stress 03 simulates the constant overburden stress in the road construction. The cyclic 'deviator stress' σ_d, which simulates the in situ stress due to traffic loading, varies between zero and a preset value at a frequency of 1 Hz. The major principal stress oi is then equal to:

$$\sigma_1 = \sigma_d + \sigma_3 \quad (1)$$

The intermediate principal stress σ_2 is equal to the minor principal stress σ_3:

$$\sigma_1 = \sigma_d + \sigma_3 \quad (2)$$

The sum of principal stresses s is equal to:

$$\theta = \sigma_1 + \sigma_2 + \sigma_3 = \sigma d + 3\sigma_3 \quad (3)$$

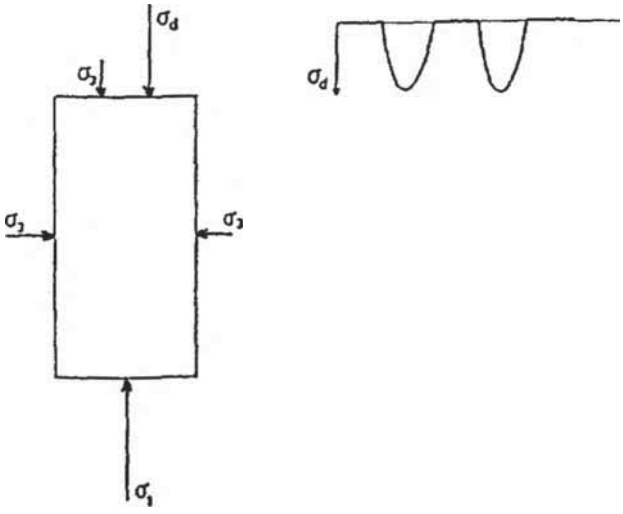


Figure 4. Stresses applied to specimen in cyclic loading triaxial tests.

The 400 mm x 800 mm triaxial apparatus (figure 5) uses a partial vacuum inside the sample to create the confining stress σ_3. A 100 kN MTS hydraulic actuator is used to apply cyclic deviator stresses σ_d to the sample.
The use of the vacuum triaxial principle eliminates the necessity of a triaxial cell and there by allows for easy accessibility of the sample and the measuring equipment during the test. Two plexiglass rings mounted on the sample at 1/3 and 2/3 of sample height respectively support four vertical LVDT's (Linear Variable Displacement Transducers) for measurement of axial deformation and two horizontal LVDT's for measurement of radial deformation.

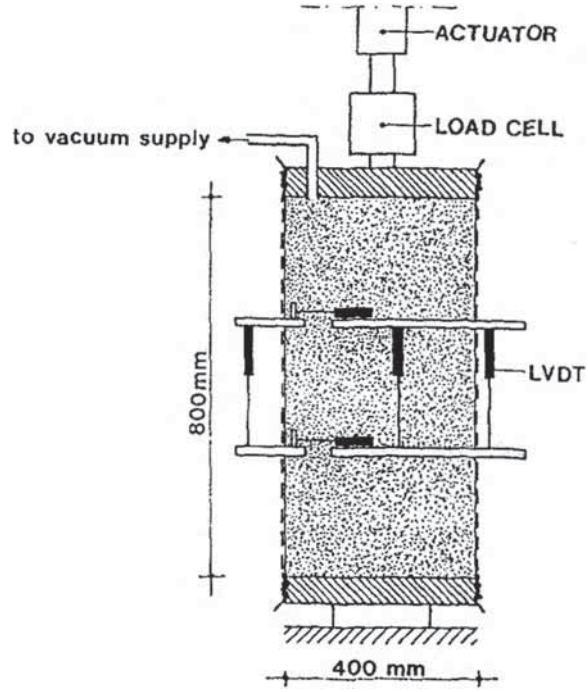


Figure 5. Outline of 400 mm x 800 mm cyclic loading triaxial apparatus.

By means of cyclic loading triaxial tests, both the resilient and plastic behaviour of the unbound materials of the test sections were determined.
For the determination of the resilient strain parameters of the materials, one triaxial sample was tested at various levels of the confining stress σ_3 and the deviator stress σ_d. The most widely known model for characterizing the resilient behaviour of unbound materials comprises the resilient modulus M_r and Poisson's ratio v, defined as:

$$M_r = \frac{\sigma_d}{\varepsilon_{a,r}} \quad (4a)$$

$$\nu = -\frac{\varepsilon_{r,r}}{\varepsilon_{a,r}} \quad (4b)$$

where: $\varepsilon_{a,r}$ - axial resilient strain of the sample
$\varepsilon_{r,r}$ - radial resilient strain of the sample

The stress-dependency of M_r is usually expressed using the equation:

$$M_r = k_1 \cdot \theta^{k_2} \quad (5)$$

where: k_1,k_2 = material parameters
θ = sum of principal stresses (eq. 3)

Figure 6 shows the M_r-θ relationships from the cyclic loading triaxial tests for the crushed sand, the crushed concrete and the Eastern Scheldt sand, applied in the concrete block test sections.

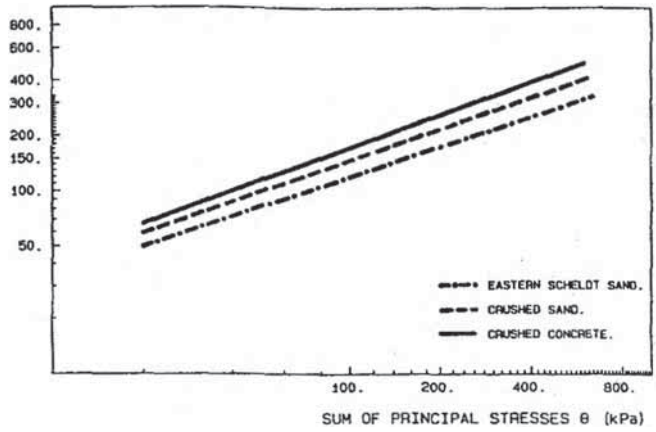


Figure 6. M_r-θ relationships for the unbound materials applied in the six concrete block test sections.

For the determination of the plastic strain parameters three samples of each material were tested at the same confining stress σ_3, with a different level of the deviator stress σ_d. The samples were loaded with up to 10^6 load applications, or until failure.
Figure 7 shows, for three different stress ratio's $n = \sigma_d/\sigma_3$, the axial permanent strain ε_a,p versus the number of load applications N for the crushed concrete and the Eastern Scheldt sand. The permanent deformation behaviour of the crushed sand was supposed to be equal to that of the crushed concrete base material.

4.2. Resilient deformation behaviour (deflections) of the test sections

For the determination of the resilient deformation behaviour of the test sections, falling weight deflection measurements were carried out regularly. In such a deflection measurement a dynamic load (loading time 0.02 s) is applied on the pavement structure by means of a circular plate with diameter ø = 300 mm. The deflections (d) have been measured at distances of 0, 0.3, 0.5, 1.0, 1.5 and 2.0 m from the centre of the loading plate (figure 8).
In the wheel track testing the concrete block test sections were subjected to 6 kN wheel loads, and therefore in the deflection measurements also a 6 kN load was applied.

In the figures 9 and 10 some test results are given.
Figure 9 shows the mean deflection curves of the various test sections at the beginning of testing (zero load repetitions) as well as at the and of testing (after 275,000 wheel load repetitions).

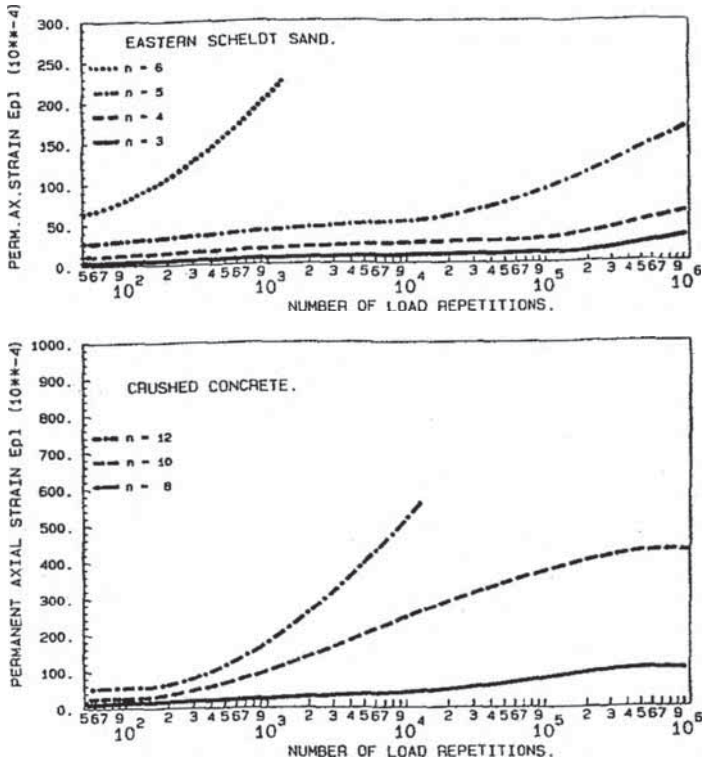


Figure 7. ε_a,p-N relationships for the unbound malerials applied in the six concrete block test sections.

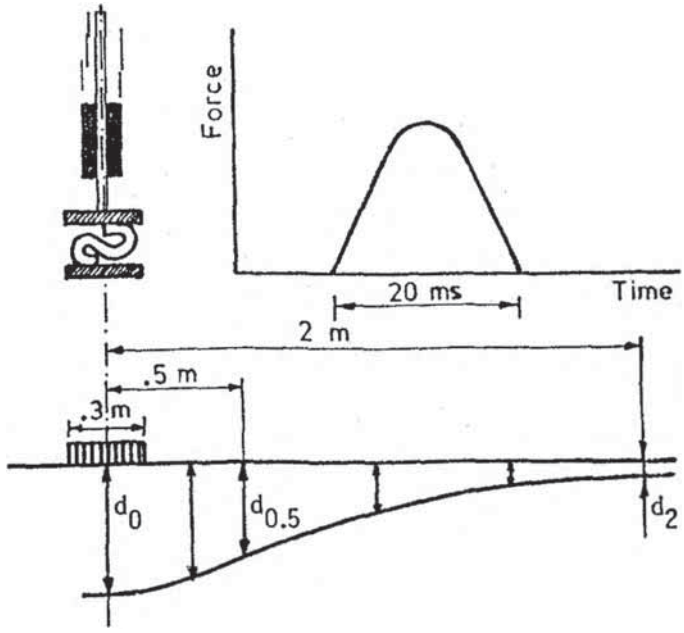


Figure 8. Outline of a falling weight deflection measurement.

In figure 10 the mean maximum deflection dg (in the load centre) of the various test sections is given as a function of the number of wheel load repetitions.
As the corresponding sections 1 and 6 (0 mm base) as well as 3 and 5 (200 mm base) showed a similar resilient deformation behaviour, both in figure 9 and figure 10 the deflections of the combined sections have been plotted.

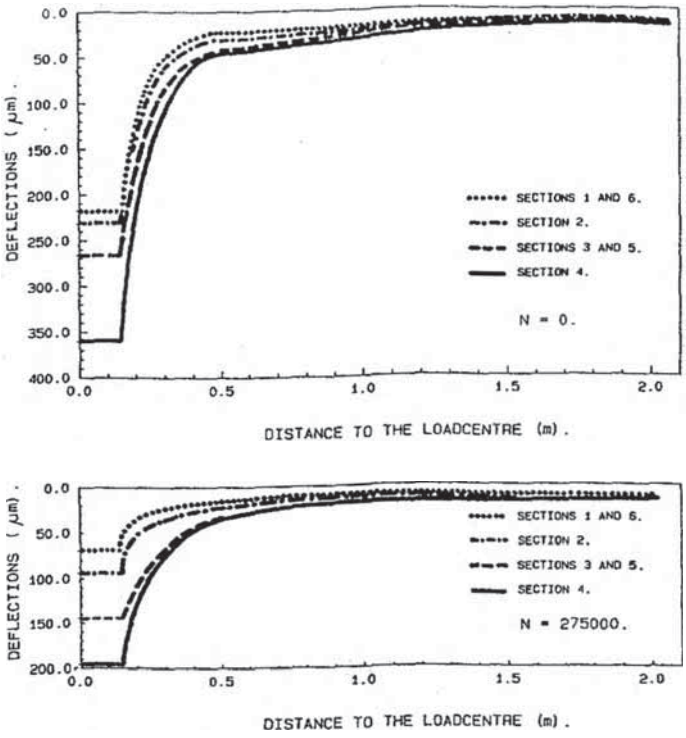


Figure 9. Mean deflection curves (due to load P = 6 kN, ø = 300 mm) of the concrete block test sections after N = 0 (above) and after N = 275,000 (below) wheel load (P = 6 kN, p = 0.6 N/mm^2) repetitions.

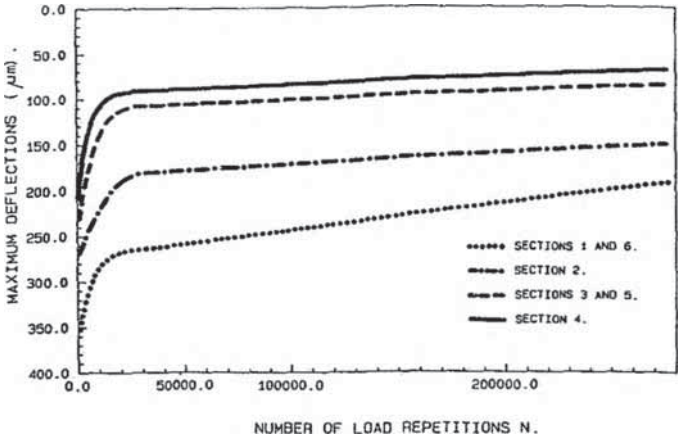


Figure 10. Mean maximum deflection d_0 (due to load P = 6 kN, ø = 300 mm) of the concrete block test sections as a function of the number of wheel load (P = 6 kN, p = 0.6 N/mm^2) repetitions.

In the figures 9 and 10 it can be observed that:
- the measured deflections decrease with increasing base thickness, which means that the load spreading capacity of concrete block pavements increases with increasing base thickness
- the measured deflections decrease (and the load spreading capacity increases) with increasing number of load repetitions: all test sections show the characteristic 'progressive stiffening' behaviour of concrete block pavements .

4.3. Permanent deformation behaviour (rutting) of the test sections

For the determination of the permanent deformation behaviour (rutting) of the test sections, level measurements were carried out regularly.
Figure 11 gives the mean cross profiles of the test sections at various numbers of applied wheel load repetitions, while figure 12 shows the progress of rutting with increasing number of load repetitions.
Also with respect to rutting, the corresponding sections 1 and 6 as well as 3 and 5 showed a simi lar behaviour.

The figures 11 and 12 show:
- the rutting behaviour of the sections 1 and 6 (without a base) is much worse than the behaviour of the sections 2 through 5 (with an unbound base of crushed concrete)
- the thickness of the unbound base only has a slight effect on the rutting behaviour of the test sections.

It can be observed in figure 12 that in test section 4 (300 mm base) the rut depth was greater than in the sections 3 and 5 (200 mm base). Most probably this unexpected result was caused by a low compaction of the bedding layer of section 4.

The progress of rutting, plotted in figure 12, can be described by the equation:

$$RD = a_{p6/0.6} \cdot (N_{6/0.6})^{b_{p6/0.6}} \qquad (6)$$

where: RD = mean rut depth (mm)
$N_{6/0.6}$ = cumulative number of (wheel track apparatus) wheel load (P = 6 kN, p - 0.6 N/mm^2) repetitions
$a_{p6/0.6}$, $b_{p6/0.6}$ = rutting coefficients for the total pavement structure, subjected to wheel loads (P = 6 kN, p = 0.6 N/mm^2)

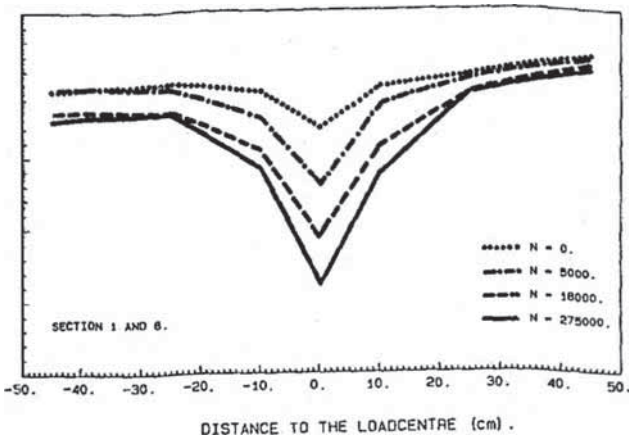
For the various test sections the calculated rutting coefficients $a_p6/0.6$ and $b_p6/o.6$, as well as the regression coefficient r, are given in table 2.

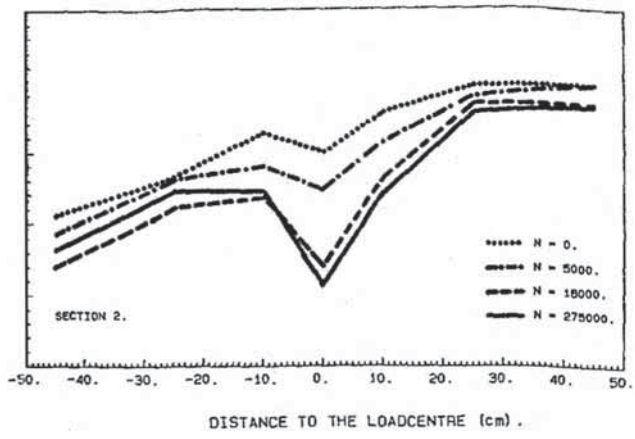
With respect to the maximum deflection cig (in the centre of the load) due to the applied wheel track apparatus loads, the following relationship was deducted by means of the theory of Boussinesq:

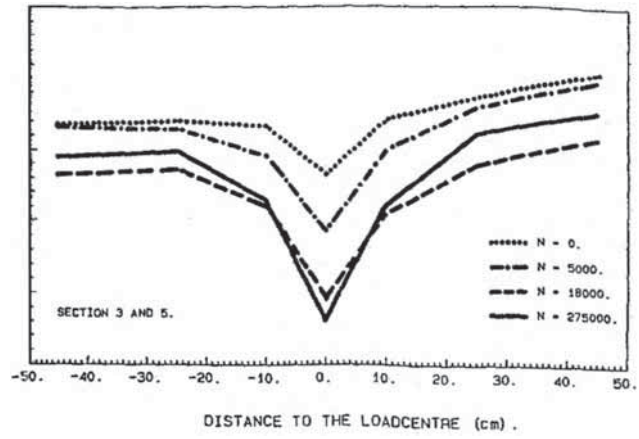
$$d_{0,6/0.6} = 2.65\ d_{0,6/\phi 300}$$

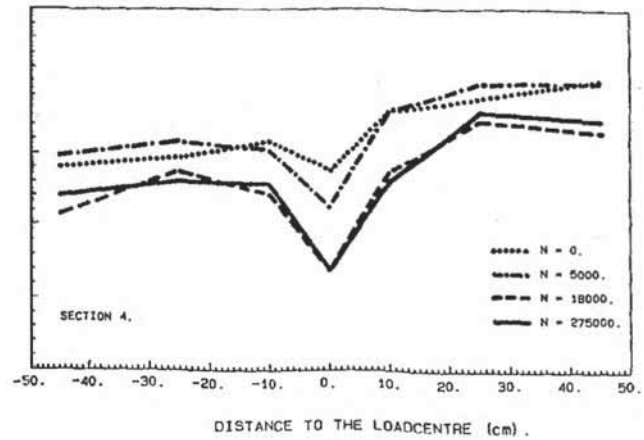
where: $d_{0,6/0.6}$ = maximum deflection due to a wheel track apparatus wheel load (P = 6 kN, p = 0.6N/mm^2)
$d_{0,6/\phi 300}$ = maximum deflection due to the falling weight load (P = 6 kN, ø = 300 mm)

From the equations 6 and 7 it follows for the number of falling weight loads:









11. Mean cross profiles of the concrete block test sections after various num - bers of wheel load (P = 6 kN, p = 0.6 N/mm^2) repetitions.

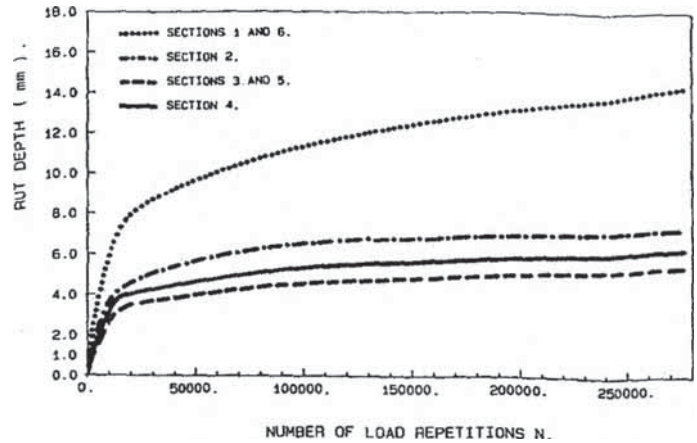


Figure 12. Mean rut depth of the concrete block test sections as a function of the number of wheel load (P = 6 kN, p = 0.6 N/mm^2) repetitions.

$$N_{6/\phi 300} = (2.65)^{\frac{1}{b_{p6/0.6}}} \cdot N_{6/0.6} \qquad (8)$$

where: $N_{6/\phi 300}$ = cumulative number of falling weight load (P - 6 kN, ø = 300 mm) repetitions
$b_{p6/0.6}$ = see equation 6
$N_{6/0.6}$ = see equation 6

The rutting of concrete block pavements, subjected to repeated falling weight loads (P = 6 kN, ø = 300 mm) can be described by the equation:

$$RD = a_{p6/\phi 300} \cdot (N_{6/\phi 300})^{b_{p6/\phi 300}} \qquad (9)$$

where: RD = mean rut depth (mm)
$N_{6/\phi 300}$ = see equation 8
$a_{p6/\phi 300}$, $b_{p6/\phi 300}$ = rutting coefficients for the total pavement structure, subjected to wheel loads (P = 6 kN, ø = 300 mm)

The rutting coefficients $a_p6/ø300$ and $b_p6/ø300$ (= $b_p6/0.6 = b_p$) of the various test sections, calculated in this way, also are given in table 2.

The number of real traffic wheel loads (for example P = 40 kN, ø = 300 mm) can be calculated from the number of falling weight loads, using an AASHTO-type load equivalency factor with respect to rutting:

$$N_{40/\phi 300} = \left(\frac{6}{40}\right)^{\frac{1}{b_p}} \cdot N_{6/\phi 300} \qquad (10)$$

where: $N_{40/\phi 300}$ = cumulative number of equivalent standard single wheel loads (P = 40 kN, ø = 300 mm)
$N_{6/\phi 300}$ = see equation 8
b_p = rutting coefficient for the concrete block pavement under consideration

section	wheel track apparatus loads (P = 6 kN, p - 0.6 N/mm^2; $N_{6/0.6}$)			falling weight loads (P = 6 kN, ø = 300 mm; $N_{6/ø300}$		equivalent standard wheel loads (P = 40 kN, ø = 300 mm; $N_{40/ø300}$)	
	$a_{p6/0.6}$	$b_{p6/0.6} = b_p$	r	$a_{p6/ø300}$	$b_{p6/ø300} = b_p$	$a_{p40/ø300}$	b_p
1 and 6	0.853	0.225	0.988	0.315	0.225	2.146	0.225
2	0.793	0.177	0.941	0.299	0.177	2.006	0.177
3 and 5	0.753	0.156	0.893	0.283	0.156	1.889	0.156
4	0.818	0.162	0.942	0.306	0.162	2.059	0.162

Table 2. Rutting coefficients a_P and b_P (with respect to the mean rut depth) of the test sections for various types of wheel loads.

The rutting of concrete block pavements, subjected to repeated equivalent standard single wheel loads, is:

$$RD = a_{p40/\phi300} \cdot (N_{40/\phi300})^{b_p} \qquad (11)$$

where: RD = mean rut depth (mm)
$N_{40/\phi300}$ = see equation 10
$a_{p40/\phi300}$, b_p = rutting coefficients for the total pavement structure, subjected to equivalent standard single wheel loads (P = 40 kN, ø = 300 mm)

The calculated rutting coefficients $a_p40/ø300$ and b_p of the various test sections also are given in table 2.

5, TWO-DIMENSIONAL FINITE ELEMENT ANALYSIS

First the behaviour of the concrete block test sections was analyzed by means of a two-dimensional ICES STRUDL finite element model (5,6,7). The thickness of the model is taken as 1 mm.
The concrete block layer is schematized by a number of indeformable 'rigid body' elements, that represent the concrete blocks, joined together by means of vertical linear springs, that represent the shear resistance of the joints (figure 13).
The spring stiffness k (N/mm) of the joints is:

$$k = \frac{G \cdot h_1 \cdot 1}{2\,w} = \frac{G \cdot h_1}{2\,w} \qquad (12)$$

where: G = shear modulus of the joints (N/mm^2)
h_1 = concrete block thickness (mm)
w = actual joint width (mm)

The concrete blocks are connected to the underlying bedding layer by means of vertical linear springs. The spring stiffness k' (N/mm) is:

$$k' = \frac{c \cdot b \cdot 1}{2} = \frac{c \cdot b}{2} \qquad (13)$$

where: c = bedding constant (N/mm^3)
b = concrete block length or width (mm), considering herringbone bond

The bedding layer, the base (if any), the sub-base and the subgrade are divided into a number of continuous elements. Each element is characterized by means of the modulus of elasticity and poisson's ratio.

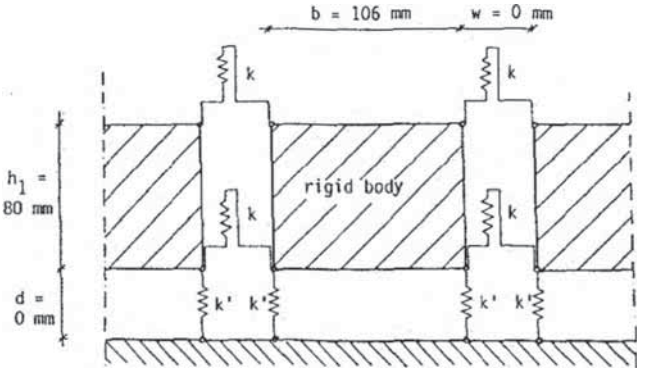


Figure 13. Two-dimensional finite element model for concrete block pa ventents.

It was assumed that the concrete block layer acts as a pure shear layer, which means that no bending moments are transmitted in the block layer and that only vertical displacements of the blocks will occur.
The two-dimensional finite element model is 'loaded' by a displacement equal to the measured maximum deflection d_0 in the centre of the load.

By means of the two-dimensional finite element representation as described above, it is possible to calculate (by means of trial and error) the combination of spring stiffnesses k and k' , in such a way that the calculated deflection curve corresponds as best as possible with the measured deflection curve.
The figures 14 and 15 show the progress of k and k' with the number of wheel load repetitions applied to the concrete block test sections.

It can be observed.in the figures 14 and 15:
- in all test sections both the joint stiffness k and the supporting stiffness k' increase with increasing number of load repetitions, which means that all sections show the characteristic 'progressive stiffening' behaviour
- in general the supporting stiffness k' increases with increasing base thickness; however, the joint stiffness k (representing the load transfer in the joints) is hardly related to the base thickness.

It is a clear disadvantage of the two-dimensional finite element representation of figure 13 that the supporting springs k' 'absorb' a great part of the load. This means that the calculated stresses, strains and displacements within the bedding layer, the base (if any), the sub-base

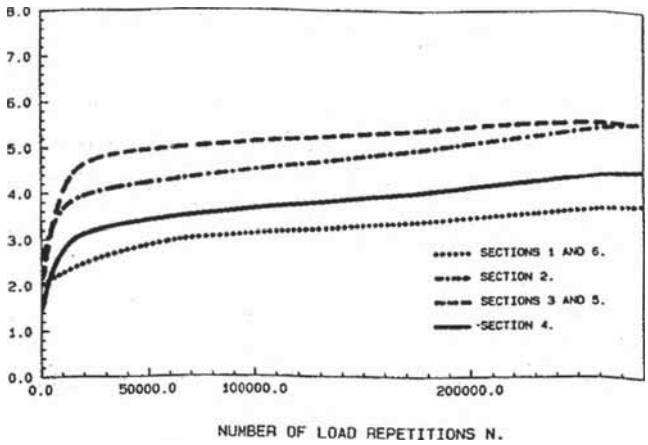


Figure 14. Joint stiffness k of the concrete block test sections as a function of the number of wheel load (P = 6 kN, p = 0.6 N/mm^2) repetitions.

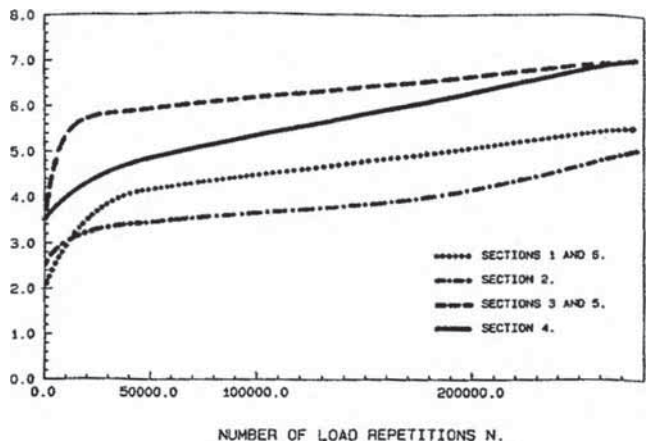


Figure 15. Support stiffness k' of the concrete block test sections as a function of the number of wheel load (P = 6 kN, p = 0.6 N/mm^2) repetitions.

and the subgrade are not reliable. Therefore for every deflection measurement the elastic compression of each of this layers was calculated by means of the linear-elastic multilayer computerprogram BISAR (8). On basis of this elastic compression, and the measured mean rut depth, for every granular material within the concrete block test sections the permanent deformation coefficients a_m and b_m can be calculated, using the 'progressive stiffening' theory developed by the Delft University of Technology (5). The basic equation of this theory is (figure IK):

$$\frac{d(\Delta h_p)}{dN} = f_1 \cdot \frac{df_2}{dN} \qquad (14)$$

where: Δh_p = permanent deformation in a layer of unbound material
f_1 = elastic compression of the layer due to the applied load
f_2 = permanent deformation relationship of the unbound material

For a granular material the 'compaction' relation f_2 is:

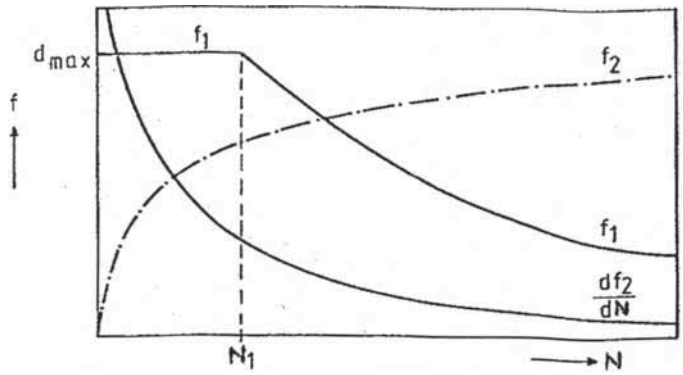


Figure 16. Schematical representation of permanent deformation functions.

$$f_2 = a_m \cdot N^{b_m} \qquad (15)$$

where: N = number of load repetitions
a_m, b_m = permanent deformation coefficients of the granular material

The elastic compression f_1 of a granular layer can be described as:

$$N \leq N_1: f_1 = d_{max} = \text{constant} \qquad (16a)$$

$$N > N_1: f_1 = p + q \cdot e^{-\log N} \qquad (16b)$$

where: N_1 = initial number of load repetitions until 'progressive stiffening' occurs
d_{max}, p, q = elastic deformation coefficients of the granular layer

The permanent deformation in a layer of granular material in a concrete block pavement is obtained by combining the equations 14, 15 and 16:

$$N \leq N_1: \Delta h_p = d_{max} \cdot a_m \cdot N^{b_m} \qquad (17a)$$

$$N > N_1: \Delta h_p = d_{max} \cdot a_m \cdot N_1^{b_m} + \qquad (17b)$$

$$a_m \cdot p \cdot (N^{b_m} - N_1^{b_m}) +$$

$$\frac{a_m \cdot b_m \cdot q}{b_m - 0.4343} (N^{b_m - 0.4343} - N_1^{b_m - 0.4343})$$

It was assumed in the 'progressive stiffening' calculations for the various concrete block test sections, investigated by means of the wheel track apparatus, that no permanent deformation occurred within the subgrade.
For the various granular layers the calculated coefficients N_1, d_{max}, p, q, a_m snd b_m are summarized in table 3 for the three types of wheel loads, distinguished in chapter 4.3.

section	layer	N_X	d_{max} (mm)	P (mm)	q (mm)	a_m	b_m
1 and 6	50 mm crushed sand bedding layer + 1100 mm sand sub-base	249,235 3,274 54	0.337 0.893 2.247	0.145 0.384 0.966	42.377 17.123 7.260	0.266 0.401 0.592	0.32 0.32 0.32
2	50 mm crushed sand bedding layer + 100 mm crushed concrete base	1,092,633 4,447 24	0.079 0.209 0.527	0.025 0.066 0.167	22.638 5.484 1.432	0.310 0.547 0.934	0.28 0.28 0.28
	1000 mm sand sub-base	1,122,434 4,542 25	0.164 0.435 1.093	0.071 0.190 0.476	39.284 9.506 2.490	0.120 0.263 0.555	0.32 0.32 0.32
3 and 5	50 mm crushed sand bedding layer + 200 mm crushed concrete base	1,344,144 2,573 7	0.104 0.276 0.693	0.020 0.053 0.133	38.585 6.764 1.308	0.277 0.599 1.247	0.28 0.28 0.28
	900 mm sand sub-base	1,584,494 3,053 8	0.104 0.276 0.693	0.029 0.078 0.197	36.747 6.459 1.242	0.072 0.201 0.530	0.32 0.32 0.32
4	50 mm crushed sand bedding layer + 300 mm crushed concrete base	502,254 1,239 4	0.123 0.326 0.820	0.015 0.038 0.098	32.403 6.337 1.336	0.444 0.902 1.766	0.28 0.28 0.28
	800 mm sand sub-base	710,093 1,703 6	0.072 0.191 0.480	0.015 0.039 0.098	19.940 3.839 0.822	0.071 0.182 0.449	0.32 0.32 0.32

figure above applies to falling weight loads (P = 6 kN, ø = 300 mm; N_6/ø300)
figure in the middle applies to wheel track apparatus loads (P = 6 kN, p = 0.6 N/mm^2; N_6/0.6)
figure below applies to equivalent standard wheel loads (P = 40 kN, ø = 300 mm; N_{40}/ø300)

Table 3. Elastic and permanent 'progressive stiffening' coefficients (with respect to the mean rut depth) of the various granular layers of the test sections for various types of wheel loads.

Starting with the test sections 1 and 6, for the sand sub-base a b_m-value of 0.32 was found; this value also was taken for the sand sub-base in the other test sections. For the crushed concrete base (including 50 mm crushed sand bedding layer) a mean b_m-value of 0.28 was calculated. As concerns the sand sub-base, the rather high a_m-value of the test sections 1 and 6 is explained by the poor initial compaction (see chapter 3). As concerns the crushed concrete base, the high a_m-value of test section 4 is due to the poor initial compaction of the crushed sand bedding layer (see chapter 4.3).

6. AXIAL-SYMMETRIC FINITE ELEMENT ANALYSIS

After the two-dimensional analysis the behaviour of the concrete block test sections was analyzed by means of an axial-symmetric ICES STRUDL finite element model.
Again the concrete block layer is schematized as a pure shear layer, that consists of a number of undeformable 'rigid bodies', joined together by vertical linear springs. The stiffness K of these springs is (figure 17):

$$d = 2 \prod r\, k \qquad (18)$$

where: k = spring stiffness according to equation 12 (N/mm per mm')
r = distance to the loadcentre (mm)

The bedding layer, the base (if any), the sub-base and the subgrade are divided into a number of continuous elements. Each element is characterized by means of the resilient modulus M_r and Poisson's ratio v, that was taken as 0.35 for all unbound materials

In this axial-symmetric finite element representation in principle the rigid body elements are fixed to the underlying bedding layer. However, with the exception of the loaded rigid body all rigid bodies are only fixed at one point to prevent tensile stresses in the bedding layer; in the other points a spring with very low stiffness k" was introduced (figure 17).

In contrast with the two-dimensional model the axial-symmetric finite element representation allows the calculation of stresses, strains and displacements within the pavement structure below the 'rigid bodies' top layer.
The axial-symmetric finite element model is loaded by a 6 kN load.

The objective of the axial-symmetric finite element calculations is to calculate the measured deflection curves, making allowance for the stress-dependent resilient deformation behaviour of the unbound materials applied in the concrete block test sections. This requires a number of iterative calculations to achieve that for each

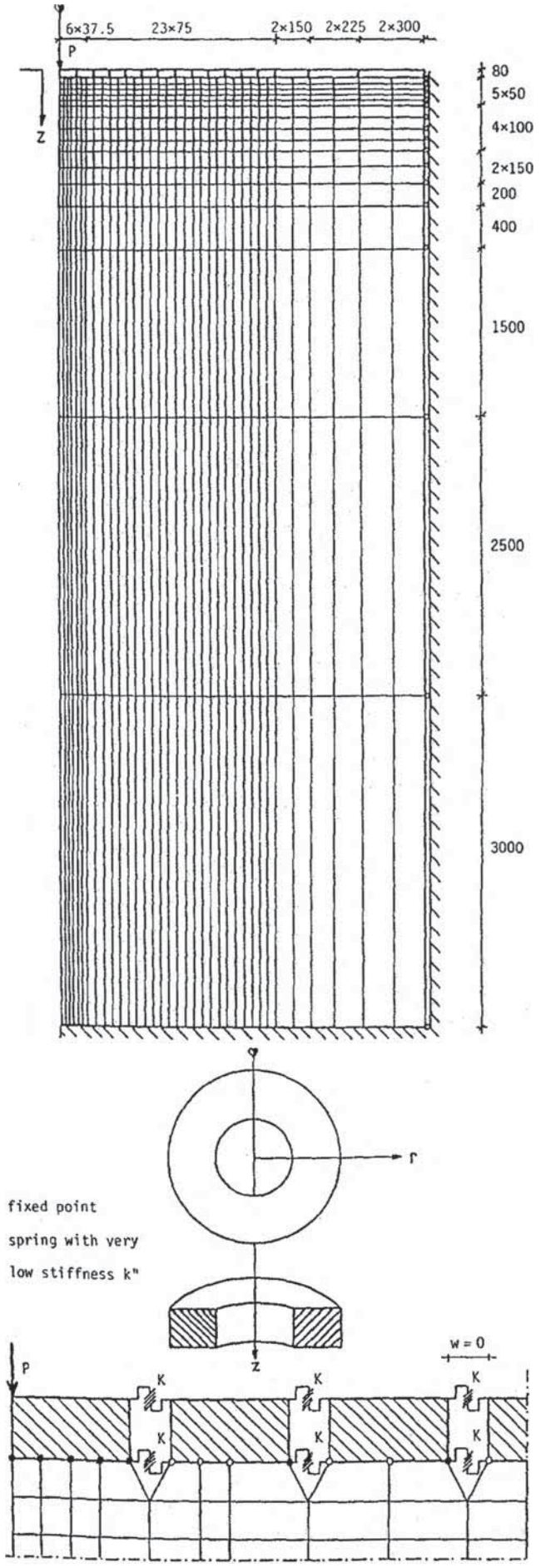


Figure 17. Axial-symmetric finite element model for concrete block pavements (dimensions in mm).

element of unbound material the input resilient modulus is in accordance with the stress-dependent modulus (equation 5 and figure 6), where the stresses include both the dynamic stresses, and the overburden stresses in the roadconstruction. These extensive calculations only were carried out for the test sections 1/6 and 3/5.
Some results of the finite element calculations are shown in the figures 18, 19 and 20.

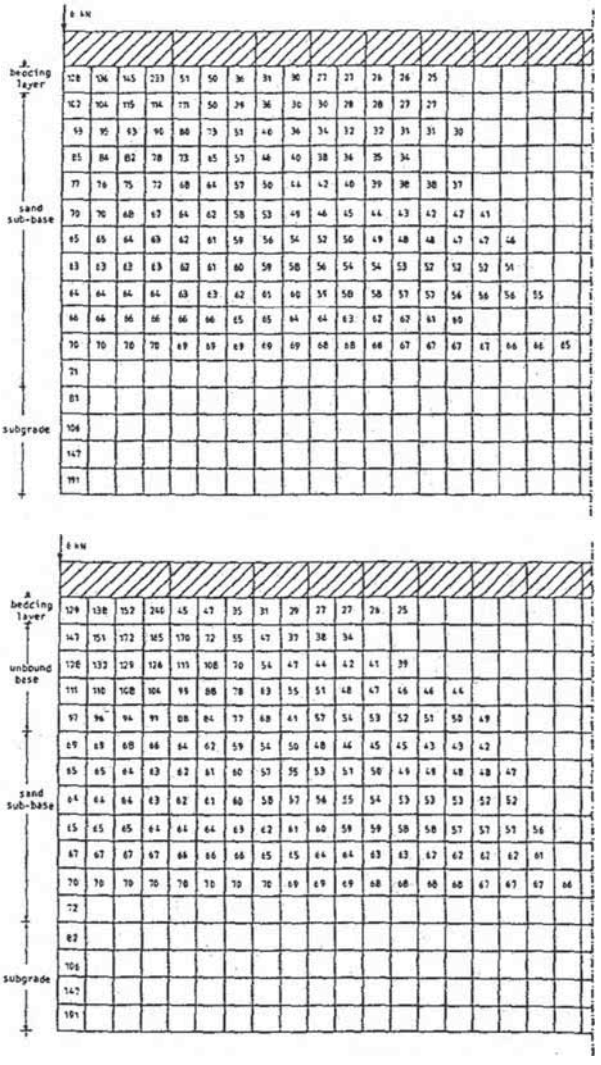


Figure 18. Stress-dependent resilient modulus M_r (MPa), according to figure 6, of each element of unbound material in the test sections 1 and 6 (above) and 3 and 5 (below); load P = 6 kN, joint stiffness k - 2.0 N/mm.

Using the M_r-θ relationships from figure 6 and the minimum joint stiffness k = 2.0 N/mm (found in the two-dimensional finite element calculati-ons, see figure 14), the measured deflection curve of the sections 1 and 6 only could be cal-culated by the axial-symmetric finite element mo-del for N = 180,000 wheel load repetitions (fi-gure 18 above). For less than 180,000 load repetitions the M_r-values of these sections had to be reduced (caused by an inferior initial compaction of the sand sub-base, see chapter 3), while for more than 180,000 load repetitions a slightly increasing joint stiffness k was found (figure 19)
Because of the good initial compaction, in the

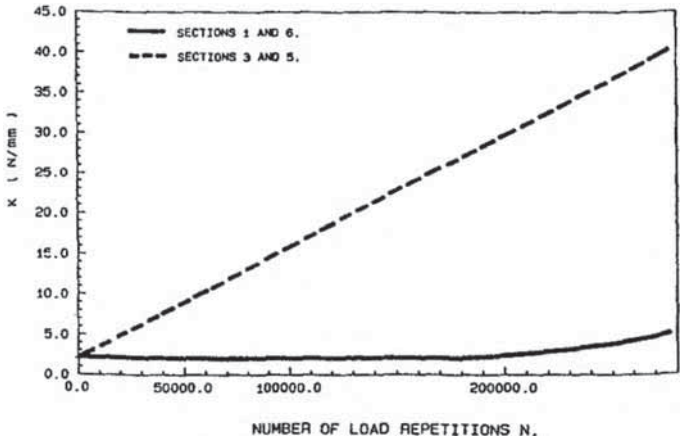


Figure 19. Calculated progress of joint stiffness k in the axial-symmetric finite element model; load P = 6 kN.

sections 3 and 5 the M_r-e relationships from figure 6 could be applied for every deflection curve. These sections showed a substantial increase of the joint stiffness k with increasing number of load repetitions (figure 19).

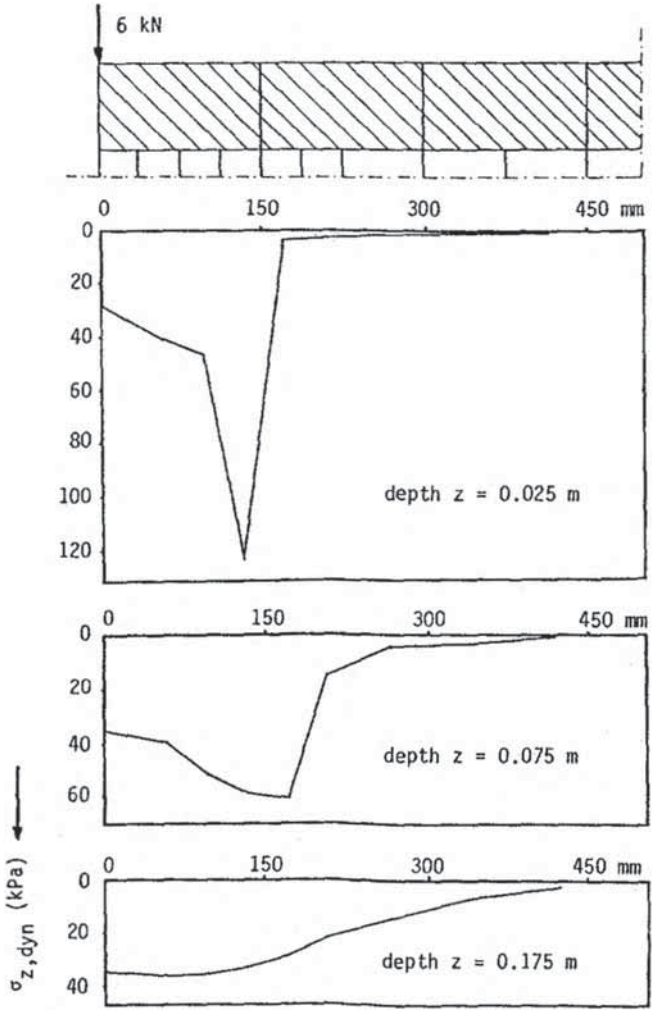


Figure 20. Vertical dynamic stresses within the test sections 1 and 6 at several depths below the concrete block layer; load P = 6 kN, joint stiffness k = 2.0 N/mm.

In figure 20 it can be observed that in case of new concrete block pavement with a rather low joint stiffness k:

- there is hardly any load transfer from the load ed concrete paving block to adjacent blocks
- directly below the loaded 'rigid body' concrete paving block the distribution of vertical dynamic stresses is very much alike the stress distribution below a very stiff foundation, with peak stresses below the edge of the loaded block
- at a depth of about 0.2 m below the concrete block layer the regular distribution of vertical dynamic stresses is reached.

At last the rutting of the test sections 3 and 5 was calculated on basis of an axial-symmetric finite element analysis.
Because of the increasing joint stiffness k with increasing number of load repetitions (figure 19), the total number of wheel load repetitions was divided into 5 periods. For each period the resilient modulus Mr of the unbound material elements (similar to figure 18) was calculated, and next the stress ratio n - oi/oz of the elements below the loaded concrete block. By means of the permanent deformation relationships of figure 7, first the permanent strain and next the permanent deformation of these elements was determined. For each period the rutting behaviour was found by adding the permanent deformation of all elements below the loaded concrete block. The actual progress of rutting was then calculated by means of superposition of the rutting behaviour per period. From figure 21 it seems that there is a very good correspondence, especially at long term, between the calculated and measured rutting on the test sections 3 and 5.

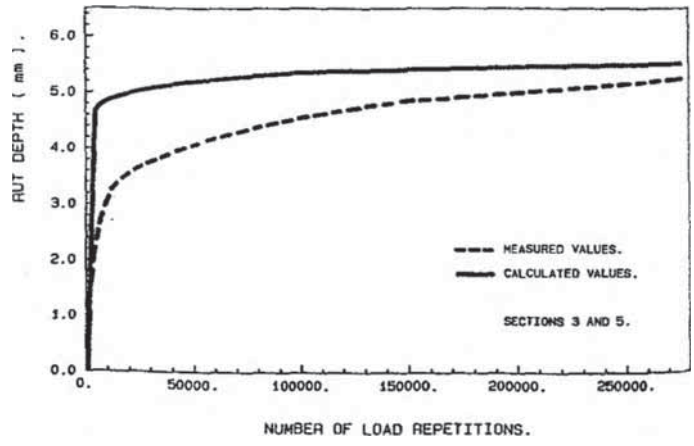


Figure 21. Comparison of the measured and calculated rutting behaviour of the test sections 3 and 5; load P = 6 kN, p = 0.6 N/mm^2.

7. CONCLUSIONS

On basis of the research into the structural behaviour of six concrete block test pavements as described in this paper, the following conclusions can be made:

1. In spite of the rather low wheel load (P = 6 kN, p = 0.6 N/mm^2), the Delft wheel track apparatus seems very applicable for the investigation of the structural behaviour, especially

rutting, of concrete block pavements.
On basis of falling weight deflection measurements a two-dimensional finite element analysis yields a rough insight into the characteristic 'progressive stiffening' behaviour of concrete block pavements. From this analysis and the measured rutting behaviour, for each granular layer of the concrete block test pavements permanent deformation coefficients can be derived to be used for design purposes (see also (9)).
A more advanced axial-symmetric finite element analysis combined with the fundamental stress-dependent resilient and permanent deformation characteristics of the applied unbound materials, in principle are the two basic components for a fundamental design method for concrete block pavements. However, this procedure takes much (computer)time, so for the time being it is more suitable for the analysis of detail problems in concrete block pavements.

REFERENCES

1. Jacobs, M.M.J. and L.J.M. Houben
Research into Concrete Block Pavements with an Unbound Base - A Comparative Investigation by means of the Delft Wheel Track Apparatus (in Dutch)
Report 7-86-200-10, Road and Railroad Research Laboratory, Delft University of Technology, Delft, 1986

2. Jacobs, M.M.J. and L.J.M. Houben
Comparative Investigation into the Structural Behaviour of Concrete Block Pavements (in Dutch)
Wegen, nr. 7/8, July/August 1987, pp. 269-276

3. Rijkswaterstaat
Requirements for Construction Materials in Highway Engineering (in Dutch)
Staatsuitgeverij, The Hague, 1978

4. Sweere, G.T.H., A. Penning and E. Vos
Development of a Structural Design Procedure for Asphalt Pavements with Crushed Rubble Base Courses
Proceedings Sixth International Conference Structural Design of Asphalt Pavements, Ann Arbor, 1987

5. Houben, L.J.M., A.A.A. Molenaar, G.H.A.M. Fuchs and H.O. Moll
Analysis and Design of Concrete Block Pavements
Proceedings Second International Conference on Concrete Block Paving, Delft University of Technology, Delft, 1984, pp. 86-99

6. Working Group D3 'Design of Small Element Pavements ' of Dutch Study Centre for Roadconstruction
Behaviour of Two Concrete Block Test Pavements on a Poor Subgrade
Proceedings Second International Conference on Concrete Block Paving, Delft University of Technology, Delft, 1984, pp. 115-128

7. Kellersmann, G.H., J. van der Klooster, G.R. Bosch, E. Beuving, A.A.A. Molenaar and H.O. Moll
Design Method for Concrete Block Pavements
Proceedings Second International Conference on Concrete Block Paving, Delft University of Technology, Delft, 1984, pp. 100-114

8. Jong, D. de, M. Peutz and A. Korswagen
Computer Program BISAR - Layered Systems under Normal and Tangential Surface Loads
External Report AMSR.0006.73, Royal/Shell Laboratory KSLA, Amsterdam, 1973

9. Working Group D3 'Design of Small Element Pavements' of Dutch Study Centre for Roadconstruction
The Dutch Design Method for Concrete Block Road Pavements
Proceedings Third International Conference on Concrete Block Paving, Rome, 1988